Research Article | Vol. 26, No. 15 | 23 Jul 2018 | OPTICS EXPRESS 18928

Optics EXPRESS

# Fiducial-aided on-machine positioning method for precision manufacturing of optical freeform surfaces

SHIXIANG WANG,[1] CHIFAI CHEUNG,[1,*] MINGJUN REN,[1,2] AND MINGYU LIU[1]

[1]*Partner State Key Laboratory of Ultra-Precision Machining Technology, Department of Industrial and Systems Engineering, The Hong Kong Polytechnic University, Kowloon, Hong Kong, China*
[2]*Robotics Institute, School of Mechanical Engineering, Shanghai Jiao Tong University, Shanghai, China*
[*]*Benny.Cheung@polyu.edu.hk*

**Abstract:** There are still significant challenges in the accurate positioning of optical freeform surfaces on the machine tool and the measurement instrument due to the high accuracy requirement and their complex shapes. This paper proposes a fiducial-aided on-machine positioning method (FAOPM) that combines on-machine measurement and off-machine measurement to precisely position optical freeform surfaces during the precision manufacturing cycle including rough machining, fine machining, measurement, and error compensation. The FAOPM makes use of fiducials which are firstly measured on a coordinate measuring machine with nanometric accuracy to generate a fiducial-aided computer aided design (FA-CAD) of the designed optical surface, then the developed on-machine measuring device obtains the accurate positions of the fiducials after remounting in the machining coordinate system. Finally the relative position of the workpiece is identified so that the associated cutting paths and compensation tool path can be easily generated. Several optical freeform surfaces were experimentally machined to prove the capability of the proposed method. The results indicate that the positions of the workpiece during the precision manufacturing and measurement cycle were precisely achieved and the form accuracy of the optical freeform surfaces was remarkable improved based on the FAOPM.



## 1. Introduction

Optical freeform surfaces have numerous applications in advanced optical systems, such as imaging, illumination, condensing light and other applications [1]. This is due to their excellent optical performance in terms of reducing size and enriching functions [2]. However, high accuracy such as sub-micrometer form accuracy and nanometric surface finish, and complex shapes bring considerable challenges for ultra-precision freeform surface machining, measurement and application processes.

To improve the form accuracy, it is necessary to compensate for the error of the workpiece after off-machine measurement in a commercial high-precision measuring device. On the other hand, with the consideration of machining efficiency, the freeform surfaces usually need to be roughly machined with a precision machine tool before being machined by ultra-precision machine tools. It is inevitable that a precise remounting process should be carried out on the ultra-precision machine tool to control the unnecessary removal of material. For a conventional rotationally symmetrical surface [3], this process is relatively easy to operate because of the distinct features. However, freeform surfaces generally possess non-rotational symmetry which makes it extremely difficult to remount the workpiece with high precision. Switching the workpiece between machining and measuring instrument can lead to re-positioning errors which limit the fabricated freeform surface accuracy while this also significantly extends the total time of production. As a result, tedious manual adjustments and special designed extra reference structures or fixtures are usually implemented when switching the workpiece among different equipment [4,5].

#330074 https://doi.org/10.1364/OE.26.018928
Journal © 2018 Received 25 Apr 2018; revised 30 Jun 2018; accepted 1 Jul 2018; published 10 Jul 2018
Corrected: 23 July 2018

Optics EXPRESS

It is interesting to note that on-machine measurement has been developed to solve the remounting problem [6,7]. Some research work involving a contact trigger probe and non-contact optical measurement approaches has been found [8,9]. However, such on-machine measurement methods may be limited by the systematic errors of the machine since the equipment for measurement is installed on the axes of the machine tool. These relatively small errors still pose considerable challenges in regard to machining ultra-precision freeform surfaces [10,11]. Some improving methods have been developed. By using off-machine commercial measurement to obtain a reference model of the machined surface, Zhang et al. [12] combined on-machine measurement (Linear Variable Differential Transformer LVDT system) to achieve the position of the remounted workpiece in the machining coordinate system, so the compensation step is then implemented, including the surface profile errors resulting from the measurement of both on-machine and off-machine models. Zhang et al. [13] mounted a fringe deflectometry system on a five-axis ultra-precision machine (Moore Nanotech 350UPL) to position the optical freeform surface in the machine tool.

Apart from the machining process, positioning problems also occur when the machined surface is aligned to the ideal surface. Both are usually embedded in different coordinate frames. Many methods are proposed to solve this problem. Jiang et al. [14] used an inscribed sphere as a global feature for fine alignment. Kong et al. [15] developed a coupled reference data method which provided additional structures like spheres and planes to carry out fast matching. Based on mean-square distance, Shaw et al. [16] used the iterative closest point algorithm and rigid body transformation for 3D shape registration. Cheung et al. [17] made use of Gaussian curvature as an intrinsic feature of the freeform surface for data matching. However, there is still a lack of an international standard for the accuracy measurement and characterization of the form accuracy of freeform surfaces [18,19].

Additional fiducials are considered to be one of the solutions to address these problems which serve as references to strengthen the measuring process. Standard balls are widely employed for the manufacturing and measurement process, but have received relatively little attention [20,21] in the manufacturing of freeform optics. As a result, a new method based on a fiducial-aided positioning method is presented here not only to obtain the accurate positions of the workpiece in different machining processes but also to strengthen the surface metrology.

## 2. Theory of the fiducial-aided on-machine positioning method (FAOPM)

Figure 1 shows the process flow of the proposed Fiducial-aided on-machine positioning method (FAOPM) which basically consists of five key processes, including a fiducial design process, an off-machine measurement process, an evaluation process, a positioning process and a machining process. Considering the conditions of design requirements, including geometric complexity of the designed surface (DS), the characteristics of machine tools and the measuring instruments, a specific fixture is designed with known distribution of fiducials using standard geometry such as a sphere as elements serving as references. A high-precision off-machine measurement device (i.e. CMM) is then employed to measure the freeform workpiece and fiducials mounted on the fixture in a thermally controlled environment. Hence, the relative position between the mounted workpiece and the fiducials is determined by the measuring device so that the fiducial-aided-CAD (FA-CAD) is generated by integrating the CAD of the DS with the measured fiducials after best fitting the designed surface to the measured workpiece. Generally, the added fiducials serve as inherent surface features of the FA-CAD which are used for precision positioning later in the manufacturing cycle.

Optics EXPRESS

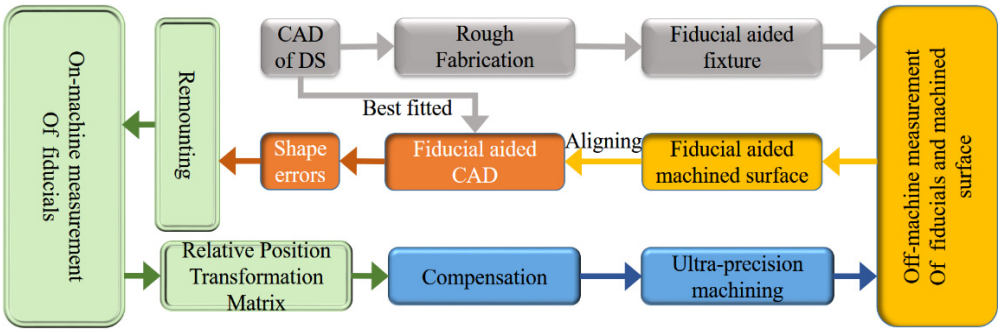


Fig. 1. Flow-process of the proposed FAOMP.

In the positioning process, the position of the re-clamped workpiece can be obtained by the developed on-machine measurement instrument. Fig. 2 shows how to position the freeform surface after remounting the workpiece. Firstly, all the fiducials are measured by the laser probe with the same sampling points. Then the FA-CAD is transformed from the reference coordinate frame to the machine tool coordinate frame (MTCF) with the aid of fiducials (references).

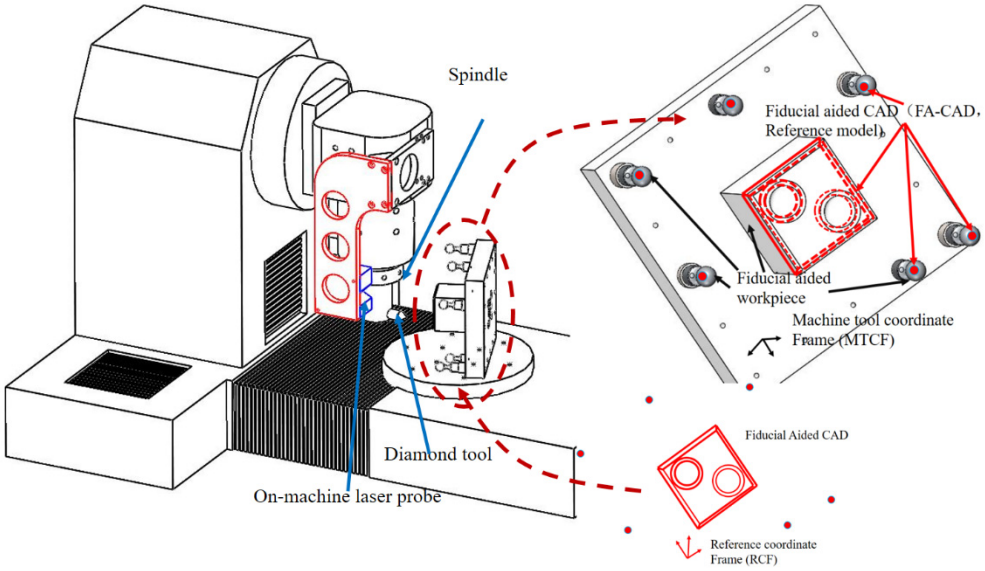


Fig. 2. Positioning the remounted workpiece by using on-machine laser probe measuring fiducials (references).

In order to transfer the fiducials and designed surface (FA-CAD) to the machining coordinate frame, a coordinate transformation matrix $\mathbf{T}$ is used which can be defined by Eq. (1).

$$\mathbf{T}(\mathbf{m}) = \begin{bmatrix} \mathrm{c}(\gamma)\mathrm{c}(\varphi) & \mathrm{s}(\gamma)c(r_y)+c(\gamma)s(\varphi)s(\phi) & \mathrm{s}(\gamma)s(\phi)-c(\gamma)s(\varphi)c(\phi) & \delta_x \\ -\mathrm{s}(\gamma)c(\varphi) & c(\gamma)c(\phi)-s(\gamma)s(\varphi)s(\phi) & c(\gamma)s(\phi)+s(\gamma)s(\varphi)c(\phi) & \delta_y \\ s(\varphi) & -c(\varphi)s(\phi) & \mathrm{c}(\varphi)\mathrm{c}(\phi) & \delta_z \\ 0 & 0 & 0 & 1 \end{bmatrix} \quad (1)$$

Optics EXPRESS

where $\mathbf{m}=\left[\phi,\varphi,\gamma,\delta_x,\delta_y,\delta_z\right]$ is a vector that consists of the translational parameters $\delta_x$, $\delta_y$ and $\delta_z$, and the rotational parameters $\phi$, $\varphi$ and $\gamma$. Besides, $c()$ and $s()$ are the functions of cosine and sine functions.

During the process of positioning the freeform workpiece on the machine tool, there are $N$ feature points in the different coordinate frames as shown as the six balls in Fig. 2, so the transferring process can be determined by non-linear programming (NLP) as Eq. (2):

$$F(\mathbf{m})=\min\sum_{i=1}^{N}\left|\mathrm{P}-\mathbf{T}\,\mathrm{P}'\right|^2 \tag{2}$$

where $\mathrm{P}'$ is the point which is located in the reference coordinate frame and $\mathrm{P}$ is the corresponding points in the machine tool coordinate frame. In order to find the global minimizer of Eq. (2), a scatter search based on a multi-start framework called OptQuest/NLP [22] is employed. (i) Firstly, all the local minimizers $\mathbf{m}$ of Eq. (2) are firstly found with a NLP solver and are sorted by $F$ from lowest to highest; (ii) Then all the $i$ which satisfy Eq. (3) in the loop over local minimizer $j$ are found; (iii) Lastly, the $\mathbf{m}(j)$ and $F(j)$ are recorded and output.

$$\begin{aligned}&|F(i)-F(j)|<=\varsigma_F*\max(1,|F(j)|)\\&|\mathbf{m}(i)-\mathbf{m}(j)|<=\varsigma_m*\max(1,|\mathbf{m}(j)|)\end{aligned} \tag{3}$$

where $\varsigma_F$ and $\varsigma_m$ are the tolerances of function and the parameters respectively.

In the machining process, the transferred FA-CAD is used to generate the tool path of the freeform workpiece by taking into consideration the machining strategy, machining parameters and tool information. The evaluated errors are then compensated for by modifying the generated NC code. Fig. 3 shows the pipeline for machining the freeform workpiece in the FAOPM.

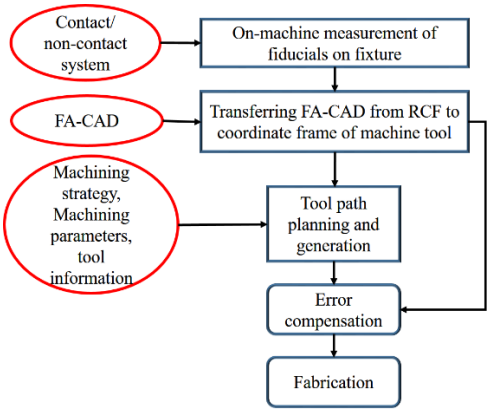


Fig. 3. The process of machining freeform surfaces in the FAOPM.

The machined workpiece is measured and characterized on a high-precision measuring instrument. Traditionally, the measured surface and designed surface embedded in different coordinate systems are aligned based on the least square method or the minimum zone method so as to evaluate the deviation between them. However, these methods possess many challenges such as uncertainty due to the lack of distinguishing inherent geometric features on freeform surfaces. In the proposed FAOPM, the alignment between the measured surface and the designed surface is done in a more robust way as shown in Fig. 4 since a FA-CAD model is constructed in the calibration and positioning process to guide the measurement process.

Optics EXPRESS

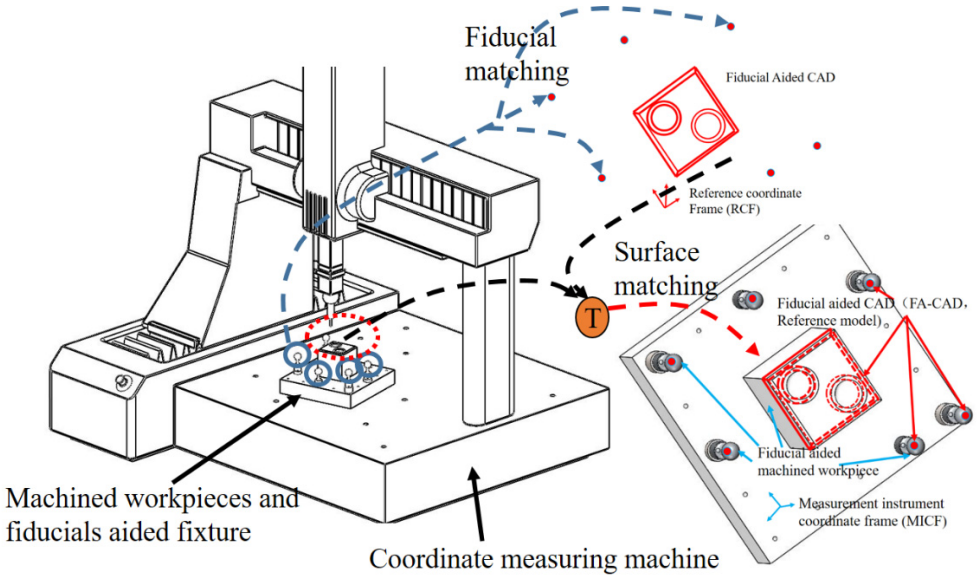


Fig. 4. Positioning the machined surface in the measurement instrument and evaluation using fiducial-aided CAD (reference model).

Figure 4 shows the measurement process of the machined freeform workpiece in the FAOPM. Firstly, the freeform workpiece and the fiducials are measured on the measuring instrument. Secondly, all known systematic errors associated in the measured data are corrected based on the standard sphere, e.g. the bending error of the probe stylus and the tip ball correction for CMM measurement. The measured fiducials in the measurement instrument coordinate frame (MICF) are then aligned to the reference datum of the FA-CAD in the RCF so as to determine the spatial parameters of coordinate transformation matrix $\mathbf{T}$ from MICF to RCF based on Eq. (2). A fiducial-aided least square method [23] is developed to carry out the surface matching process. The measured surface in MICF is subsequently transformed to the RCF and the form error of the workpiece is evaluated by determining the deviation of the machined surface from the designed surface in FA-CAD by Eq. (4) as follows:

$$Ef_{eva,i} = \left(\mathbf{S}\left(u_i, v_i\right) - \mathbf{TQ}_i\right) \cdot \bar{n}(u_i, v_i) \tag{4}$$

where $\mathbf{S}$ is the design surface; $Ef_{eva,i}$ is the error of measured surface at $\mathbf{Q}_i$; $\mathbf{S}\left(u_i, v_i\right)$ is the projection of $\mathbf{TQ}_i$ on $\mathbf{S}$; $\bar{n}(u_i, v_i)$ is the unit normal vector of $\mathbf{S}\left(u_i, v_i\right)$. Finally, the evaluated $Ef_{eva}$ are used to calculate the selected surface parameters to examine the conformance of the workpiece with specifications. Fig. 5 shows the flow chart of the surface form evaluation.

Optics EXPRESS

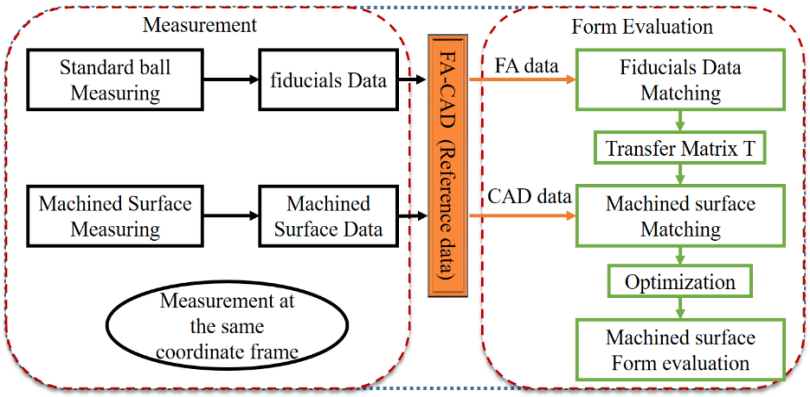


Fig. 5. The flow chart of the measurement of freeform surface in the FAOPM.

## 3. Configuration and calibration of the measurement system

As aforementioned, the primary concept of the FAOPM is that the positioning is based on the measuring accuracy of fiducials in the on-machine measurement instrument. As a result, a reliable and accurate on-machine measurement system is critical to the proposed method. Sensors such as touch trigger probes, scanning sensors and laser displacement sensors can be employed in on-machine measurement [24]. Recently, the workpiece measurement and error compensation system probe by using a linear variable differential transformer sensor measuring the position errors have been widely used on the ultra-precision turning machine [12,25]. One drawbacks of this technique is that the centering errors of the probe tips of the sensors could be relatively large. Other approaches such as mounting an atomic force microscope on an ultra-precision machine tool have also made remarkable achievements [26] with sub-nanometer resolution although limited by its small measuring range (only several hundred micrometers). In addition, some optical methods, including white light interferometer system and phase measuring deflectometry have been used to measure the profile or wavefront of reflective or refractive surfaces [13,27]. These approaches seem to be sensitive to the quality of the environment as well as the geometric complexity of the freeform optics. Due to the proposed method for measuring the freeform surface in the on-machine process, this study developed a measuring system which mounts a Keyence LK-laser scanner on a five-axis ultra-precision freeform raster milling system (the Freeform 705G, from Precitech Inc. in USA, as shown in Fig. 6) to measure the references such as standard balls and cones.

Optics EXPRESS

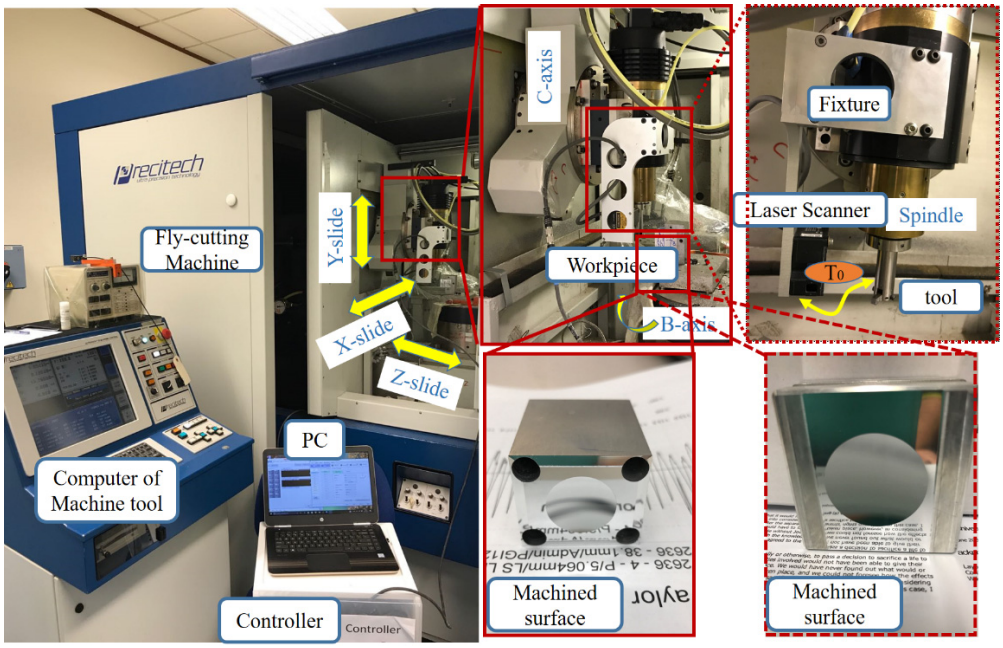


Fig. 6. Development of an on-machine measurement system on an ultra-precision raster milling machine and the machined surfaces for calibration.

Figure 6 shows the configuration of the whole on-machine measurement system. A personal computer with integrated operating software is connected to the controller which is used to transfer signals from the laser scanner. Moreover, the laser scanner is fixed on a designated fixture mounted on the main spindle so that it can be moved along with the Y-slide of the machine tool. $\mathbf{T}_0$ is the transformation matrix denoting translation and rotation deviation of the two coordinate frames between the machine tool and the on-machine measurement device. Although the fixture is designed to hold the laser probe in a particular location, some factors such as material deformation and clamping fixture may generate errors. Furthermore, the geometric errors of the machine tool and mounted laser scanner are also non-ignorable error sources. Much research work has been conducted to investigate the errors of multi-axis machine tools [28,29]. In order to calibrate the developed measuring system, two surfaces, one consisting of a slope, plane and convex sphere, and the other composed of a plane and a larger convex sphere were machined in the fly-cutting machine and then measured by the laser scanner. On the other hand, a ∅9.997 mm standard ball calibrated in a CMM was also inspected and the maximum measuring error was 0.00431 mm.

## 4. Simulation study

To test the performance of the proposed FAOPM, some simulations were implemented on software (MATLAB 2015) in an Intel Core i7 CPU 3.60GHz PC with 16GB of RAM. Firstly, two freeform surfaces (a continuous smooth surface and a sinusoidal surface) were simulated to analyze the accuracy and robustness of the proposed method in the surface matching process. Secondly, the remounting accuracy in the machining process was analyzed by adding on-machine measurement errors and geometrical errors.

### *4.1 Simulation for measurement of freeform surfaces*

The freeform surface matching process is usually formulated as an optimization problem as shown in Eq. (5) in which it is necessary to find the homogeneous coordinate transformation

Optics EXPRESS

matrix composed of six parameters $\mathbf{m} = \left[\phi, \varphi, \gamma, \delta_x, \delta_y, \delta_z\right]$, the first three rotation parameters and the last three translation parameters.

$$\min \sum_{i=1}^{N} \left| \mathrm{P}_i - \mathbf{T}\mathbf{Q}_i \right|^2 \tag{5}$$

where $\mathbf{Q}_i$ and $\mathrm{P}_i$ are the measured points and the related corresponding point in the reference coordinate frame. $\mathbf{T}$ is the transformation matrix which has been defined by Eq. (1).

Equation (5) is calculated by the robust nonlinear least squares algorithm in [23]. Figure 7 shows the measured points and the designed surface before matching and after matching.

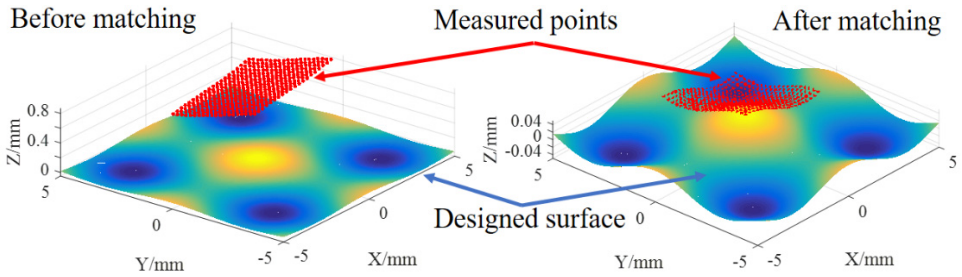


Fig. 7. Matching the measured points to the designed surface.

Two freeform surfaces in which one of them was a continuous smooth surface A while the other was a sinusoidal surface B were designed as shown in Eq. (6) and Eq. (7)

$$\begin{aligned} z &= 50(x/50)^3 + 50(x/50)^3 \\ x &\in [-5,5], \mathrm{y} \in [-5,5] \end{aligned} \tag{6}$$

$$\begin{aligned} z &= 0.025\cos(x) + 0.025\cos(y) \\ x &\in [-5,5], \mathrm{y} \in [-5,5] \end{aligned} \tag{7}$$

Three designated fiducials (standard spheres) mounted on a steel-made fixture were distributed around the designed surface. The coordinates of the ball centers were (−10, 10, 0.1), (10, 10, −0.1), (0,-10, 0), in units of mm. Geometrical errors 0.7 μm (Gaussian distributions) and other 0.3 μm caused by determining the centers of the fiducials were added to the three balls. The measured points were obtained by transferring the sampled points on the designed surface with any known six parameters $\mathbf{m}_1$ as shown in Table 1. Two thousand five hundred points were sampled on the surface with spacing of 0.2 mm in the x, and y direction, respectively.

**Table 1. Six parameters for obtaining measured surface**

| $\mathbf{m}_1$ | Values |
|---|---|
| $\phi$ | 28.6479° |
| $\varphi$ | 28.6479° |
| $\gamma$ | 28.6479° |
| $\delta_x$ | 5 mm |
| $\delta_y$ | −5 mm |
| $\delta_z$ | 1 mm |

The simulated results for the two surfaces are detailed in Table 2. Δ denotes the deviations of the six parameters between the vector $\mathbf{m}_1$ and that obtained by using the

Optics EXPRESS

FAOPM. As shown in Table 2, two error values named root-mean-square (RMS) value and peak-to-valley (height (PV) value, were used as parameters to evaluate the form accuracy. The CPU time to search the corresponding points on the designed surface and match the two coordinate frames was 0.018 s for surface A and 0.013 s for surface B. It is interesting to note that the matching process was converged after only one iteration.

**Table 2. Simulated deviations of the parameters and the surface profile**

| $\mathbf{m}_1$ | Values, A | Values, B |
|---|---|---|
| $\Delta\phi$ | 0.00146° | 0.00701° |
| $\Delta\varphi$ | 0.00675° | 0.00017° |
| $\Delta\gamma$ | –0.00719° | –0.00119° |
| $\Delta\delta_x$ | –0.000129 mm | 0.000491mm |
| $\Delta\delta_y$ | 0.0008053 mm | 0.0010648 mm |
| $\Delta\delta_z$ | –0.000735 mm | 3.49e-05mm |
| *Errors (RMS)* | 1.32e-06 μm | 3.55e-06 μm |
| *Errors (PV)* | 3.05e-06 μm | 1.17e-05 μm |

A: the smooth surface $z = 50(x/50)^3 + 50(x/50)^3$; B: the sinusoidal surface $z = 0.025\cos(x) + 0.025\cos(y)$

As shown in Table 2, both of the two surfaces could be positioned well with tiny errors of the six spatial parameters. The rotational transformation errors were up to 0.00719° while the translational transformation errors were less than 1.06 μm. Smooth surface A had the better form accuracy of less than 0.003 nm deviations both in PV value and RMS value than the arrayed-structure surface B. However, the six transformation parameters were insensitive to the different surfaces although the surface curvature varied significantly. It should be considered that the fiducials served as the intrinsic surface features. On the other hand, with the aid of the fiducials, the relatively big transformation vector $\mathbf{m}_1$ was found with a high accuracy in a more robust way by avoiding the bad initial values.

### *4.2 Simulation for remounting the workpiece*

The accuracy of the FAOPM in the remounting process was verified through the Monte Carlo method. Besides the errors added to the centers of the balls as mentioned above, several unavoidable uncertainty contributors were considered to be added in the on-machine measurement process as shown in Table 3.

**Table 3. Uncertainty error contributors in the on-machine process**

| Uncertainty errors | Values (μm, Gaussian distribution) |
|---|---|
| Laser probe | 0.2 |
| Determination of the centers | 0.3 |
| Deflection of the fixture (caused by the different temperature between the on-machine and off-machine measurement) | 0.4 |
| Geometric error | 0.5~6 |

The geometric error was considered to be the major error source in the on-machine measurement system. Hence, the magnitude of error ranging from 0.5 μm to 6 μm was used to find out the positioning accuracy and also to identify the relationship between positioning errors and the main contributing geometric errors. There were a total of 3,000 trials using the Monte Carlo simulation method. In each Monte Carlo trial, the original coordinates of the balls with added errors in the last simulation in the off-machine measuring process were transformed to the on-machine coordinate frame with the known $\mathbf{m}_2$ (88.9, 5.25, 25.35, –5, 5,

Optics EXPRESS

10). The units are the same as for $\mathbf{m}_1$. The Gaussian errors resulting from the uncertainty errors were then added to the fiducials which were considered as the reference points in the machine tool measurement frame. Fig. 8 shows the errors of the six spatial parameters with respect to the different standard deviation (SD) of the geometric error of the on-machine measurement system while Fig. 9 gives the standard deviation. Both of them are the results after three repeated measurements.

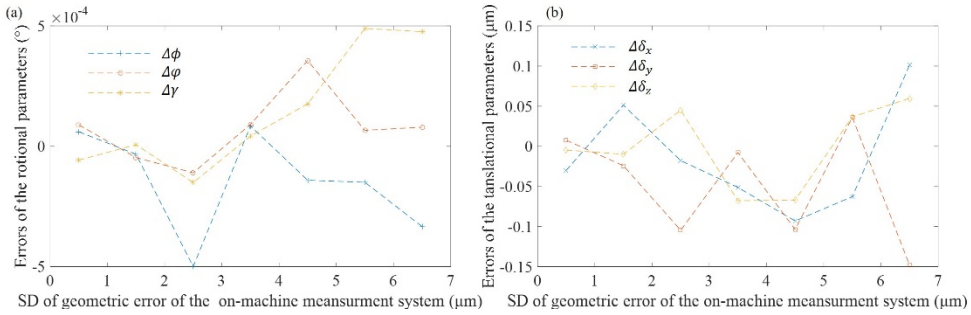


Fig. 8. Errors of (a) the rotational parameters and (b) translational parameters under different geometric error of the on-machine measurement system.

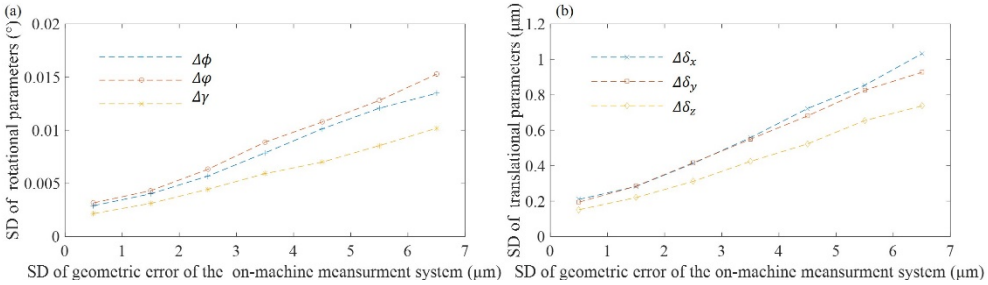


Fig. 9. Standard deviation of (a) rotational parameters and (b) translational parameters under different geometric error of the on-machine measurement system.

As shown in Fig. 8, the deviations between the found transformed six parameters and the given $\mathbf{m}_1$ shows a small fluctuation of ± 0.0005 ° for rotational parameters and ± 0.15 μm for translational parameters along with the increasing geometric errors. In addition, the deviations increase sharply when the geometric error is larger than 5 μm. In contrast, the standard deviations (SD) of the six spatial parameters see a stable increase from about 0.003° to 0.015° and from 0.2 μm to approximately 1 μm for the rotational and translational parameters respectively. In other words, the uncertainty of the FAOPM is around 10% of the geometric error of the on-machine measurement system. These simulation results indicate that the FAOPM is able to achieve sub-micrometer positioning accuracy in machine tools where the geometric error is less than 6.5 μm.

## 5. Experimental study

An optical freeform surface was employed to test the accuracy of the proposed positioning approach. A compensation experiment was carried out to verify the effectiveness of the FAOPM. The designed surface is described as Eq. (8)

$$z = (-1/250)x^2 + (1/92000)x^4 - (1/25)y^2 \qquad x \in [-15,15], y \in [-5,5] \tag{8}$$

Optics EXPRESS

As shown in Fig. 10, a quadrate fixture made of steel with dimensions of 10 mm (height) ×140 mm (width) × 140 mm (length) was used to fix the square workpiece and fiducials. Three calibrated spheres were mounted and surrounded the workpiece with different heights. They were made of $Si_3N_4$. Table 4 shows the center positions of all the spherical fiducials. The calibrated diameter of the spherical fiducial was 9.997 mm. The cube aluminum (Al6061) workpiece with the designed surface which had undergone rough cutting in a MIKRON UCP 600 Vario RTT machine tool had the dimensions of 48 mm ×48 mm × 48 mm.

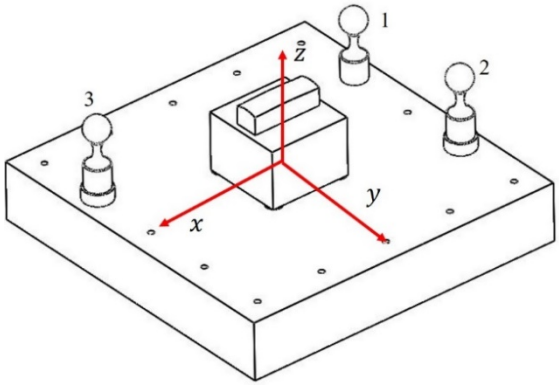


Fig. 10. Quadrate fixture and the fiducials with the pre-processed workpiece.

**Table 4. Calibrated positions of the ball center in the designed surface**

| Ball | X (mm) | Y (mm) | Z (mm) |
|---|---|---|---|
| 1 | –59.917128 | –29.993525 | 24.033117 |
| 2 | –59.650974 | 29.386402 | 28.909344 |
| 3 | 60.162073 | –29.800622 | 28.924582 |

### *5.1 Measurement repeatability of the on-machine system*

Since the designed fiducials serve as reference datum, the accuracy of the relative position of the fiducials is very important. Hence, the high measurement repeatability on the newly developed measurement system should be guaranteed. It is assumed that a ball center in the measurement coordinate frame is $q_{i,j,k}$ where $i$, $j$ and $k$ are the identifiers for the ball, the repetition and the direction, respectively. All three spheres $N_i = 3$ were measured $N_j = 3$ times. For each end of the measurement, the laser was turned off and turned on after a few minutes. A total number of 40 points were sampled on the ball. The mean ball position for each ball was calculated as well as the standard deviations (SD) in the $k=x,y,z$ direction. Hence, a pooled standard deviation (PSD) was calculated for all balls. Eqs. (9) and (10) give the formulas.

$$\bar{q}_{i,j,k} = \frac{1}{N_j}\sum_{j=1}^{N_j} q_{i,j,k}; \qquad \Delta q_{i,j,k} = q_{i,j,k} - \bar{q}_{i,j,k}; \qquad d_{i,j,k} = \| \Delta q_{i,j,k} \| \tag{9}$$

$$SD_{i,j,k} = \sqrt{\frac{\sum_{j=1}^{N_j} d^2{}_{i,j,k}}{(N_j - 1)}} \qquad PSD_{i,j,k} = \sqrt{\frac{\sum_{i=1}^{N_i} (N_j - 1) SD^2{}_{i,j,k}}{\sum_{i=1}^{N_i} (N_j - 1)}} \tag{10}$$

Table 5 shows that the largest PSD in the $k=x,y,z$ direction is up to 0.41 μm and the overall PSD is 0.34 μm. The results indicate that the repeat measured errors are acceptable.

Optics EXPRESS

**Table 5. PSD values of the repeat measurement**

| Direction | *x* | *y* | *z* | Overall |
|---|---|---|---|---|
| PSD (μm) | 0.36 | 0.41 | 0.25 | 0.34 |

### *5.2 Positioning and machining the surface*

As aforementioned, the developed on-machine measurement system was used to transform the FA-CAD into the machining coordinate frame. First, the original points of the machine tool coordinate frame (MTCF) were set after the workpiece was mounted. Second, the three reference fiducials were measured by sampling 40 points on each ball in the measurement instrument coordinate system (MICF). Hence, the FA-CAD was transformed into MICF by using the transformation matrix obtained through fiducials. Thirdly, the CAD was transformed from MICF to the MTCF through the known vector $\mathbf{T}_0$ obtained in the calibration section. Finally, the tool path could be generated. Table 6 shows the machining parameters of raster milling. Fig. 11 shows the machining process in the ultra-precision raster milling (UPRM) while Fig. 12 shows the measuring process in the CMM, Werth Videocheck from Germany.

**Table 6. Machining parameters of raster milling**

| Parameters | Value |
|---|---|
| Spindle speed (rmp) | 4000 |
| Feed rate (μm /min) | 20 |
| Depth of cut (μm) | 10, 5, 2 |
| Swing distance (mm) | 28.48 |
| Step distance (μm) | 50 |
| Tool nose radius (mm) | 0.518 |
| Cutting strategy | Horizontal cutting |

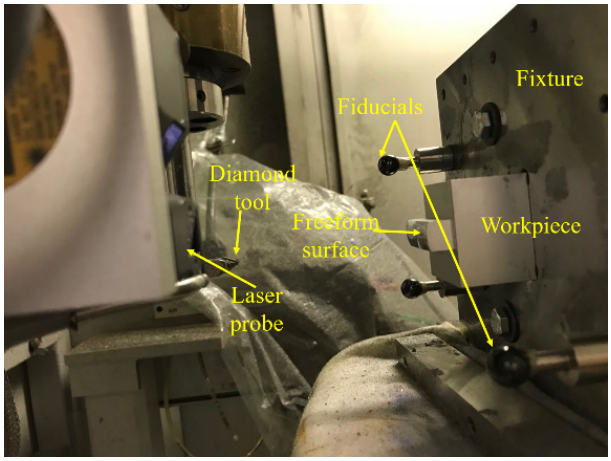


Fig. 11. Configuration for machining the freeform surface.

Optics EXPRESS

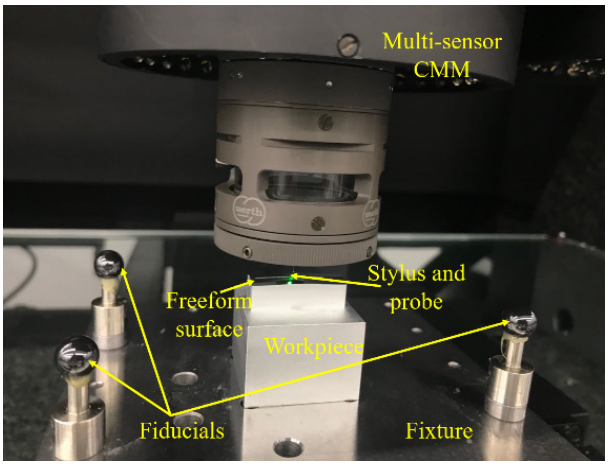


Fig. 12. Measuring the workpiece by multi sensor CMM.

A total of 1,200 points and 20 points were sampled on the machined surface and the fiducial ball, respectively. Fig. 13 shows the machined surface and its form error map after using fiducials to carry out the matching process.

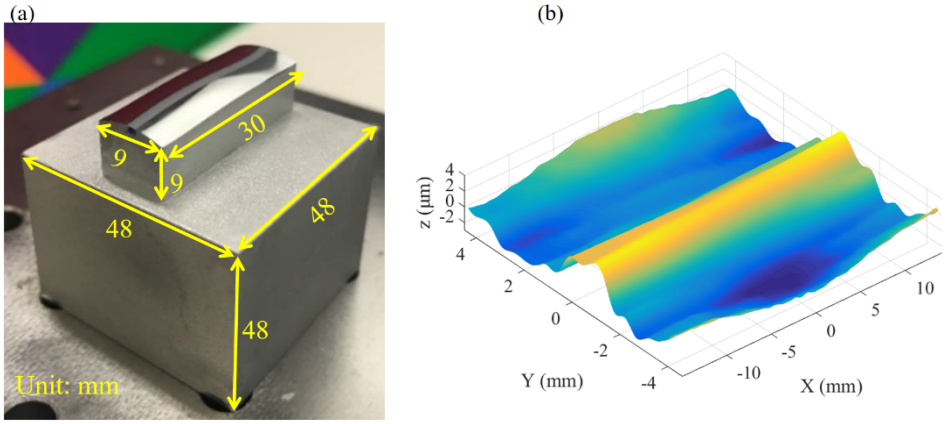


Fig. 13. (a) Machined surface and (b) the 3D error map of the surface.

As shown in Fig. 13(b), there is a relatively large form error between the machined surface and the designed surface. The peak-to-valley height (PV) was calculated to be 6.7 μm and the root-mean-square (RMS) value was 1.61 μm. Many factors result in the profile errors in UPRM, such as spindle inclination error [30], spindle vibration tool wear [31,32] and machine structural errors. Hence, it is necessary to carry out compensation of the machining process so as to enhance the form accuracy of the freeform surface.

### *5.3 Compensation machining*

In this process, the workpiece was remounted and further machined to complete the compensation of surface form error. The compensation strategy is summarized as follows: the FA-CAD was firstly transformed to the MTCF (the same as in the machining process) by using the fiducials. The 3D error map of the machined surface obtained above was then transformed to the MTCF. Further, the B-spline surface was used to generate the error map so as to extract consistent points used to generate tool path. Fig. 14(a) shows the source path and the generated compensation path. Since there were only small differences between the two

Optics EXPRESS

paths and the high accuracy of the positioning process, the cutting depth was set to 2 μm to guarantee the accuracy. In the final step, the form accuracy of the machined surface after compensation was inspected on the CMM and evaluated by the fiducial-aided surface matching method. The 3D topography of the form error is displayed in Fig 14(b).

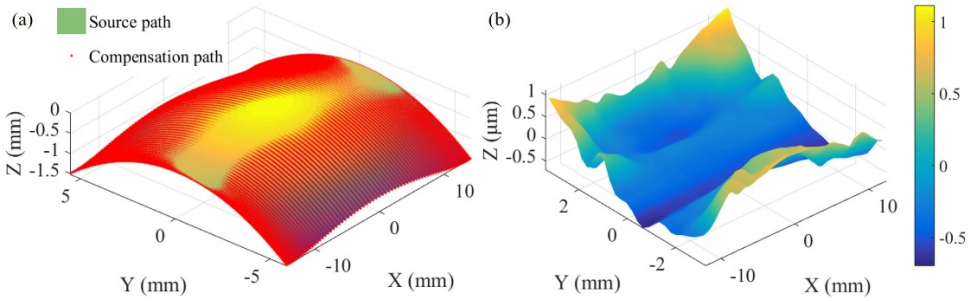


Fig. 14. (a) The source path and the revised compensation path (b) 3D topography of the form error of the surface after compensation.

To enhance the reliability of the measurement, the machined surface was sampled at 2,800 points, namely 70 × 40 in $x$ and $y$ directions respectively. As shown in Fig. 14(b), the PV value height was calculated as 1.81 μm and the RMS value was about 0.34 μm. The improvement in PV height and in RMS was significantly large, up to 78.9% (from 1.61 μm to 0.34 μm) and 73% (from 6.7 μm to 1.80 μm) respectively. This experimental result demonstrates that the FAOPM is effective in positioning the freeform surface and is capable of remarkably improving the form accuracy.

### *5.4 Sampling strategy discussion*

In order to measure and form characterize the optical freeform surfaces, it is necessary to employ an appropriate sampling strategy which involves the sampling point numbers and spacing so that the sampled points can fully represent the measured surface. A sampling strategy is considered as a major contributor to the measurement uncertainty. Measuring errors could be caused if the number of sampling points are inadequate or sampling distribution is unreasonable, especially when complex curvatures or shape of local features are contained in the surface. In the present study, a blind sampling method [33] was employed which uniformly samples the dataset from the measured surfaces in the x and y directions without considering the characteristics of the geometry both in the simulation and the experimental measurement. In the simulation study, in order to fully represent the machined surface, relatively small sampling spacing was chosen and the sampling point numbers were determined by the dimension of the surface.

In the experimental measurement, the number of sampling points were usually determined by the measurement instrument (i.e. CMM) with consideration of its resolution and time of measurement. Taking into consideration the dimensions of the workpiece, the sampling spacing can be easily determined. It is interesting to note that there is no need to sample the same number of points in the simulation and the experimental measurement. In the compensation process, adequate points (2,800 points) were sampled to guarantee the accuracy of measurement and compensation tool path generation. In other words, the blind sampling strategy is an appropriate method for flat optical surface (F-theta surface) and little effect was caused in the measurement and compensation study.

## 6. Conclusion

A novel positioning method which makes use of the designed fiducials (standard spheres) is presented for machining ultra-precision freeform surface and matching the machined surface

Optics EXPRESS

to the designed surface. The fiducial-aided CAD (FA-CAD) not only serves as an intrinsic surface feature but also interconnects the different coordinate frames among on-machine, off-machine measurement system and the designed coordinate system. The developed fiducial-aided on-machine positioning method (FAOPM) has the capability of measuring freeform surfaces with high measurement repeatability and accuracy. The results of the two simulations prove that the FAOPM not only possesses sub-micrometer positioning accuracy although the geometric error of the machine tool is several micrometers, but also can perform evaluations with higher robustness and effectiveness than by the traditional least square method when the bad initial values are used. Furthermore, the experimental results demonstrate the accuracy and effectiveness of the proposed FAOPM, as highlighted in the following technological merits.

(i) The FAOPM is a promising approach to minimize the remounting errors caused by complicated manual operations and to compensate for the form errors resulting from other factors such as vibration and geometric error.

(ii) The FAOPM is easily realized in the compensation machining process by combining off-machine measurement with the on-machine measurement system despite the positioning accuracy being influenced by the geometric error of the machine tools.

(iii) The FAOPM is capable of aligning the machined surface with the designed surface which are free from any traditional surface matching process such as least square or minimum zone method on the condition of high measurement accuracy (sub-micrometer) of the on-machine measurement system.

(iv) The FAOPM has great potential for realizing precision manufacturing optical products among different machine tools (cutting, milling and polishing).

## Funding

PhD studentship (project account code: RUEN) from The Hong Kong Polytechnic University.

## Acknowledgments

The work described in this paper was mainly supported by a grant from the Research Grants Council of the Government of the Hong Kong Special Administrative Region, China (Project No.: PolyU 15202814). The authors would also like to express their sincere thanks for the financial support provided by the Research Office of the Hong Kong Polytechnic University (Project No.: BBX7).

## References

1. F. Fang, X. Zhang, A. Weckenmann, G. Zhang, and C. Evans, “Manufacturing and measurement of freeform optics,” CIRP Ann. Manuf. Tech. **62**(2), 823–846 (2013).
2. W. Lee, S. To, and C. Cheung, *Design and advanced manufacturing technology for freeform optics*, (The Hong Kong Polytechnic University).
3. W. B. Lee, C. F. Cheung, W. M. Chiu, and T. P. Leung, “An investigation of residual form error compensation in the ultra-precision machining of aspheric surfaces,” J. Mater. Process. Technol. **99**(1-3), 129–134 (2000).
4. F. Niehaus, S. Huttenhuis, and A. Pisarski, “Fabrication and measurement of freeform surfaces using an integrated machining platform,” in *Freeform Optics*, (Optical Society of America, 2013), FW1B. 4.
5. S. Scheiding, C. Damm, W. Holota, T. Peschel, A. Gebhardt, S. Risse, and A. Tünnermann, “Ultra-precisely manufactured mirror assemblies with well-defined reference structures,” in *SPIE Astronomical Telescopes + Instrumentation*, (International Society for Optics and Photonics, 2010), 773908.
6. W. Gao, J. Aoki, B.-F. Ju, and S. Kiyono, “Surface profile measurement of a sinusoidal grid using an atomic force microscope on a diamond turning machine,” Precis. Eng. **31**(3), 304–309 (2007).
7. S. Moriyasu, Y. Yamagata, H. Ohmori, and S. Morita, “Probe type shape measuring sensor, and NC processing equipment and shape measuring method using the sensor,” (Google Patents, 2003).
8. F. J. Chen, S. H. Yin, H. Huang, H. Ohmori, Y. Wang, Y. F. Fan, and Y. J. Zhu, “Profile error compensation in ultra-precision grinding of aspheric surfaces with on-machine measurement,” Int. J. Mach. Tools Manuf. **50**(5), 480–486 (2010).
9. H. Ohmori, Y. Watanabe, W. M. Lin, K. Katahira, and T. Suzuki, “An ultraprecision on-machine measurement

Optics EXPRESS

system," in *Key Engineering Materials*, (Trans Tech Publ, 2005), 375–380.
10. W. Gao, M. Tano, T. Araki, S. Kiyono, and C. H. Park, "Measurement and compensation of error motions of a diamond turning machine," Precis. Eng. **31**(3), 310–316 (2007).
11. W. Gao, J. C. Lee, Y. Arai, Y. J. Noh, J. H. Hwang, and C. H. Park, "Measurement of slide error of an ultra-precision diamond turning machine by using a rotating cylinder workpiece," Int. J. Mach. Tools Manuf. **50**(4), 404–410 (2010).
12. X. Zhang, Z. Zeng, X. Liu, and F. Fang, "Compensation strategy for machining optical freeform surfaces by the combined on- and off-machine measurement," Opt. Express **23**(19), 24800–24810 (2015).
13. X. Zhang, L. Jiang, and G. Zhang, "Novel method of positioning optical freeform surfaces based on fringe deflectometry," CIRP Ann.- Manuf. Tech. (2017).
14. X. Jiang, P. Scott, and D. Whitehouse, "Freeform surface characterisation-a fresh strategy," CIRP Ann. Manuf. Tech. **56**(1), 553–556 (2007).
15. L. Kong, C. Cheung, S. To, W. Lee, and K. Cheng, "Measuring optical freeform surfaces using a coupled reference data method," Meas. Sci. Technol. **18**(7), 2252–2260 (2007).
16. L. Shaw and A. Weckenmann, "Automatic registration method for hybrid optical coordinate measuring technology," CIRP Ann. Manuf. Tech. **60**(1), 539–542 (2011).
17. C. Cheung, L. Kong, and M. Ren, "Measurement and characterization of ultra-precision freeform surfaces using an intrinsic surface feature-based method," Meas. Sci. Technol. **21**(11), 115109 (2010).
18. M. J. Ren, C. F. Cheung, L. B. Kong, and X. Jiang, "Invariant-feature-pattern-based form characterization for the measurement of ultraprecision freeform surfaces," IEEE Trans. Instrum. Meas. **61**(4), 963–973 (2012).
19. Y. Li and P. Gu, "Free-form surface inspection techniques state of the art review," Comput. Aided Des. **36**(13), 1395–1417 (2004).
20. K. Medicus, J. D. Nelson, and M. Brunelle, "The need for fiducials on freeform optical surfaces," in *Optical System Alignment, Tolerancing, and Verification IX*, J. Sasian and R. N. Youngworth, eds. (Spie-Int Soc Optical Engineering, Bellingham, 2015).
21. M. Brunelle, J. Yuan, K. Medicus, and J. D. Nelson, "Importance of Fiducials on Freeform Optics," in *Optifab 2015*, J. L. Bentley and S. Stoebenau, eds. (Spie-Int Soc Optical Engineering, Bellingham, 2015).
22. Z. Ugray, L. Lasdon, J. Plummer, F. Glover, J. Kelly, and R. Martí, "Scatter search and local NLP solvers: A multistart framework for global optimization," INFORMS J. Comput. **19**(3), 328–340 (2007).
23. S. Wang, C. F. Cheung, M. Ren, and M. Liu, "Fiducial-Aided Robust Positioning of Optical Freeform Surfaces," Micromachines (Basel) **9**(2), 52 (2018).
24. D. Li, C. F. Cheung, M. Ren, L. Zhou, and X. Zhao, "Autostereoscopy-based three-dimensional on-machine measuring system for micro-structured surfaces," Opt. Express **22**(21), 25635–25650 (2014).
25. S. Smith, R. Wilhelm, B. Dutterer, H. Cherukuri, and G. Goel, "Sacrificial structure preforms for thin part machining," CIRP Ann. Manuf. Tech. **61**(1), 379–382 (2012).
26. A. Shibuya, Y. Arai, Y. Yoshikawa, W. Gao, Y. Nagaike, and Y. Nakamura, "A spiral scanning probe system for micro-aspheric surface profile measurement," Int. J. Adv. Manuf. Technol. **46**(9-12), 845–862 (2010).
27. E. Olesch, C. Faber, R. Krobot, R. Zuber, and G. Häusler, "Quantitative Deflectometry Challenges Interferometry," in *Fringe 2013: 7th International Workshop on Advanced Optical Imaging and Metrology*, W. Osten, ed. (Springer Berlin Heidelberg, Berlin, Heidelberg, 2014), pp. 907–910.
28. N. Huang, Q. Bi, Y. Wang, and C. Sun, "5-Axis adaptive flank milling of flexible thin-walled parts based on the on-machine measurement," Int. J. Mach. Tools Manuf. **84**, 1–8 (2014).
29. S. Ibaraki, T. Iritani, and T. Matsushita, "Calibration of location errors of rotary axes on five-axis machine tools by on-the-machine measurement using a touch-trigger probe," Int. J. Mach. Tools Manuf. **58**, 44–53 (2012).
30. G. Zhang, S. To, and G. Xiao, "A novel spindle inclination error identification and compensation method in ultra-precision raster milling," Int. J. Mach. Tools Manuf. **78**, 8–17 (2014).
31. S. Zhang and S. To, "The effects of spindle vibration on surface generation in ultra-precision raster milling," Int. J. Mach. Tools Manuf. **71**, 52–56 (2013).
32. G. Zhang, S. To, and G. Xiao, "The relation between chip morphology and tool wear in ultra-precision raster milling," Int. J. Mach. Tools Manuf. **80**, 11–17 (2014).
33. S. D. Phillips, B. Borchardt, W. T. Estler, and J. Buttress, "The estimation of measurement uncertainty of small circular features measured by coordinate measuring machines," Precis. Eng. **22**(2), 87–97 (1998).